Check for updates

ChemSusChem

Research Article
doi.org/10.1002/cssc.202402038

Chemistry Europe
European Chemical Societies Publishing

www.chemsuschem.org

Sustainable Formate Production via Highly Active CO_2 Hydrogenation Using Porous Organometallic Polymer with Ru-PNP Active Sites

Hongjin Park[+],[a] Kwangho Park[+],[b] Ung Lee,[b] and Sungho Yoon*[a]

Efforts to combine the advantages of homogeneous catalysts in terms of activity with the ease of separation process offered by heterogeneous catalysts continue to be actively pursued in the field of catalyst development. Heterogeneous catalysts were synthesized from Ru-MACHO organometallic compounds, recognized for their high hydrogenation catalytic activity linked to the active site of the Ru-PNP motif, through direct polymerization utilizing the Friedel-Crafts reaction. These catalysts were then applied for the conversion of greenhouse gas carbon dioxide (CO_2) into formate via hydrogenation, exhibited with a record-high turnover frequency of 31,700 and a productivity of 36,100 $kg_{formate}/(kg_{catalyst}\cdot d)$. Furthermore, the facile separation characteristics and recyclability of the heterogeneous catalysts were confirmed.

Introduction

The increase in atmospheric CO_2 concentration is widely recognized as a major reason of global warming, prompting extensive research aimed at mitigating further CO_2 accumulation and reducing its existing levels.[1] One promising approach within this effort is the development of methods for converting CO_2 into valuable chemical resources that are integral to our daily lives.[6] Notable among these chemicals are carbon monoxide (CO) and formic acid, which can be produced via two-electron reductions, formaldehyde via a four-electron reduction, and methanol via a six-electron reduction.

Formic acid, in particular, stands out as it can be synthesized through the reaction of one molecule of CO_2 with one molecule of H_2, yielding no by-products and thus achieving 100% atom economy.[8–9] This high efficiency makes the CO_2-to-formic acid conversion a highly attractive target for researchers. As a result, significant attention has been directed towards developing and optimizing catalytic processes that facilitate this transformation.[13]

Because the direct reaction of $CO_2(g)$ with $H_2(g)$ to generate formic acid(l) is thermodynamically unfavorable,[18] typically, it is conducted in aqueous solution in the presence of a base, leading to the thermodynamically favored formation of formate rather than formic acid. To enhance the reaction rate, a catalyst capable of efficient hydrogenation in aqueous basic solutions is required (Table S1).

Despite the long history of hydrogenation catalyst development, many existing catalysts function primarily in organic solvents.[22] Recently, a few of hydrogenation catalysts effective in aqueous media have been reported for CO_2-to-formate conversion.[32, 37] However, these catalysts are often homogeneous, posing challenges in separating the catalyst from the products after reaction.[38, 40] Advancements have been made in developing heterogeneous hydrogenation catalysts for CO_2-to-formate conversion, overcoming these separation issues.[13, 44] Although demonstration projects utilizing these newly developed heterogeneous catalysts for CO_2-to-formic acid conversion are underway,[16] the activity of these heterogeneous catalysts still falls short of the long-established homogeneous hydrogenation catalysts. Therefore, further research is needed to enhance the activity of heterogeneous catalysts.

In the case of homogeneous catalysts, hydrogenation catalysts that include nitrogen (N) atoms in their ligands have progressively evolved to incorporate phosphine (P) atoms in the ligands.[23–39] After over several decades of research and development, Ru-MACHO catalyst series, which features a PNP motif, has been reported to exhibit excellent performance as a hydrogenation catalyst.[32,54] Notably, within the Ru-MACHO series, catalysts with ligands having four phenyl groups (PPh_2) attached to the P atoms have demonstrated extraordinary catalytic hydrogenation activity, achieving a maximum turnover number (TON) of 210,000 in the CO_2 to formate reaction.[32] However, despite this excellent activity, these homogeneous catalysts still face limitations in separation from the products and reuse, necessitating research into their heterogenization.

To enhance the potential for direct industrial application while maintaining the activity of the developed homogeneous catalyst during the heterogenization process, a relatively

[a] *Department of Chemistry, Chung- Ang University, Dongjak-gu, Seoul, Republic of Korea*
[b] *Clean Energy Research Center, Korea Institute of Science and Technology (KIST), Seongbuk-gu, Seoul, The Republic of Korea*
***Correspondence:** Sungho Yoon, Department of Chemistry, Chung- Ang University, 84 Heukseok-ro, Dongjak-gu, Seoul 06974, Republic of Korea. Email: sunghoyoon@cau.ac.kr*
[+] *These authors contributed equally to this work.*

Supporting Information for this article is available on the WWW under https://doi.org/10.1002/cssc.202402038

© 2024 The Authors. ChemSusChem published by Wiley-VCH GmbH. This is an open access article under the terms of the Creative Commons Attribution Non-Commercial License, which permits use, distribution and reproduction in any medium, provided the original work is properly cited and is not used for commercial purposes.

© 2024 The Authors. ChemSusChem published by Wiley-VCH GmbH

straightforward method for creating porous heterogeneous catalysts was explored. The approach involved connecting the phenyl groups present in the ligand of the Ru-MACHO PPh_2 catalyst with alkyl groups via a Friedel-Crafts alkylation reaction (FCR). The resulting porous heterogeneous Ru-MACHO PPh_2 catalysts, with a high active content retention (10.4 wt%), exhibited a remarkable catalytic rate of up to 31,700 turnover frequency (TOF), resulting in a productivity of 36,100 ($kg_{formate}$/($kg_{catalyst}$·d). Additionally, multiple recycling experiments demonstrated that the catalyst maintained its activity, enabling the hydrogenation of carbon dioxide to formic acid. This demonstrates the potential of the PNP-type porous organometallic polymer (POMP) as a heterogeneous catalyst for CO_2 utilization to mitigate global warming.

Results and Discussion

The POMP structured Ru-MACHO heterogeneous catalyst, referred to hereafter as Ru-MACHO-POMP (**1**), was synthesized by directly heterogenizing the homogeneous Ru-MACHO catalyst under solvothermal reaction conditions (Figure S1).[56] As depicted in Scheme 1, during the synthesis, the Ru-MACHO catalyst underwent a reaction in dichloromethane, with $AlCl_3$ as the Lewis acid catalyst, facilitating Friedel–Crafts alkylation, leading to the formation of Ru-MACHO-CH_2Cl (Scheme 1). Further alkylation occurred, promoting inter-crosslinking and polymerization among the Ru-MACHO molecules. After completing the reaction, the catalyst was isolated by simple filtration. The obtained catalyst powder exhibited a dark brown color (Figure S1). The as-prepared **1** powder is insoluble in all commonly used organic solvents, originating its heterogeneous nature, and maintains the color even in air indicating its stability in ordinary stock condition.

The particle size of **1** was calculated to be ca. 25 (±5) μm, exhibiting irregular morphology through field emission scanning electron microscopy (FE-SEM) analysis (Figure 1a). Subsequently, powder X-ray diffraction (PXRD) measurements revealed an extreme broad peak at $2\theta = 12.6°$, reiterating the amorphous nature of the prepared **1** (Figure S2). To examine the distribution of Ru in the synthesized particles, energy-dispersive X-ray spectroscopy (EDS) was performed, revealing Ru sites are uniformly distributed in the powder catalyst (Figure 1b). The porosities of the prepared catalysts were assessed by N_2 adsorption and desorption isotherm measurements. The **1** prepared using the solvothermal method displayed a type-I isotherm, demonstrating the predominant presence of a microporous structure (Figure 1c; Figure S3). Based on the results calculated using the Brunauer–Emmett–Teller (BET) theory, the synthesized **1** contains a specific surface area of 580 $m^2 g^{-1}$ and a mean pore diameter of 1.9 nm. This suggests that **1**, which is advantageous for the adsorption of substrates such as CO_2 and hydrogen,[59] will facilitate the smooth approach of formate, the product, to the active site.

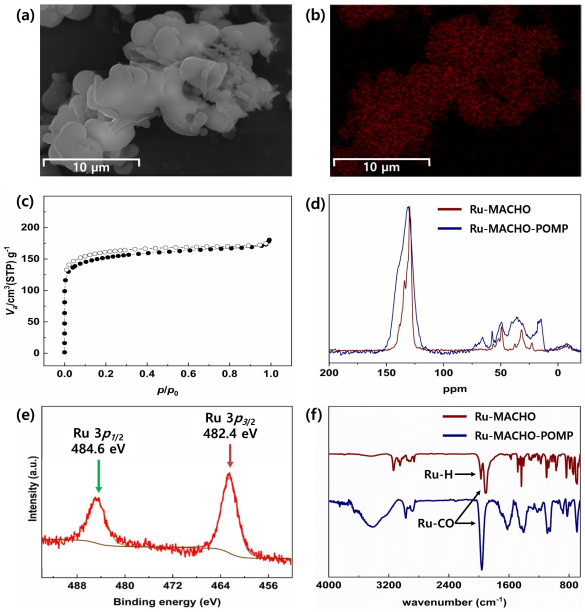
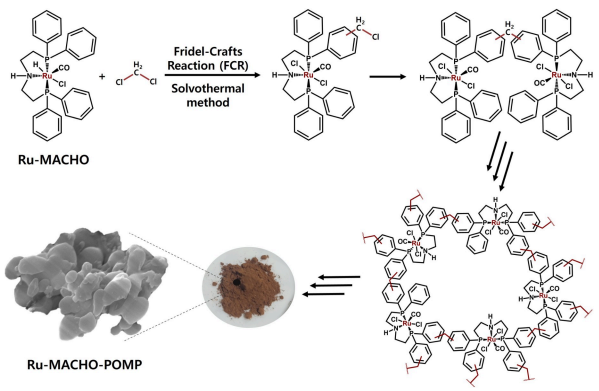


Figure 1. (a) FE-SEM image of the **1**; (b) EDS mapping (Ru) image of the **1**; (c) N_2 isotherm graph of the **1**; (d) ^{13}C CP MAS ssNMR spectra of Ru-MACHO and **1**; (e) deconvoluted XPS graph of the **1** in the Ru 3*p* binding energy region; (f) FT-IR spectra of Ru-MACHO and **1**.

Elemental analysis (EA) and ^{13}C solid-state nuclear magnetic resonance (ssNMR) spectroscopy were performed to investigate whether crosslinking occurred using -CH_2- in dichloromethane as a linking agent for the formation of **1**. Compared with the homogeneous Ru-MACHO analog, **1** exhibited a significantly higher C/N ratio of 33.80 (Table S2). This indicates that a large amount of -CH_2- groups, derived from CH_2Cl_2, are included as a crosslinking agent connecting the Ru-MACHO units. ^{13}C ssNMR measurements were also conducted on the as prepared **1** (Figure 1d). The peaks of phenyl rings in homogeneous Ru-MACHO were commonly observed at $\delta = 150–120$ ppm. Additionally, the CH_2 peaks of the -NH-CH_2-CH_2-P- structure included in the MACHO ligand were observed at 50 and 30 ppm. Similarly, in **1**, the carbon region of PPh_2 was observed at 150–120 ppm, and an increased intensity of CH_2 peaks at 20–50 ppm was also observed. This is reported as the -CH_2- bridge region formed during polymerization via FCR.[60] Peaks of Ph-CH_2- bridges were observed at $\delta = 20–50$ ppm. Along with the higher C/N ratio of EA, the high intensity of the Ph-CH_2-Ph bridge in



Scheme 1. The synthetic route of heterogeneous Ru-MACHO-POMP (**1**) from homogeneous Ru-MACHO.

© 2024 The Authors. ChemSusChem published by Wiley-VCH GmbH

1864564x, 2025, 5, Downloaded from https://chemistry-europe.onlinelibrary.wiley.com/doi/10.1002/cssc.202402038 by Chung-Ang University, Wiley Online Library on [11/05/2026]. See the Terms and Conditions (https://onlinelibrary.wiley.com/terms-and-conditions) on Wiley Online Library for rules of use; OA articles are governed by the applicable Creative Commons License

^{13}C ssNMR spectrum for **1** compared to that of homogeneous Ru-MACHO indicate crosslinking between the phenyl rings of the Ru-MACHO monomers.

To analyze the quantity, oxidation state, and coordination sphere of Ru atoms included in the prepared **1**, subsequent analyses such as inductively coupled plasma optical emission spectrometry (ICP-OES), X-ray photoelectron spectroscopy (XPS), and Fourier transform infrared (FT-IR) spectroscopy were conducted (Figure 1). The Ru content in **1** was determined to be 10.4 wt% through ICP-OES measurements. This indicates that the synthesized heterogeneous catalyst consists of more than 63 wt% homogeneous Ru-MACHO catalyst. To determine the oxidation states of the active sites of the Ru catalyst, XPS measurements were conducted (Figure 1, e and S4). The deconvoluted peak of Ru $3d_{5/2}$ exhibited a binding energy of 281.3 eV (Figure S4), and the deconvoluted peaks of Ru $3p_{1/2}$ and Ru $3p_{3/2}$ exhibited binding energies of 484.6 and 482.4 eV, respectively (Figure 1e). This indicates that the binding energies of Ru 3p and Ru 3d correspond to the Ru oxidation state 2+.[65, 72] According to previous results of heterogenizing Ru-MACHO, it was reported that Ru–H is substituted by Ru–Cl in the presence of an excess amount of $AlCl_3$ during the reaction process.[65, 74] The anticipated structural changes in the active sites during polymerization were investigated using FT-IR spectroscopy (Figure 1f). The active site of the Ru-MACHO catalyst contains Ru–H and Ru-CO, exhibiting vibration peaks at 1970 cm^{-1} (Ru–H) and 1910 cm^{-1} (Ru-CO), respectively (Figure 1f).[75] The measured FT-IR spectrum exhibited only the vibrational peak of Ru-CO (1950 cm^{-1}), without the presence of a peak corresponding to Ru–H, indicating the complete substitution of Ru–H in Ru-MACHO with Ru–Cl via the solvent-knitting method.[65, 74] Therefore, according to previous analyses, the **1** was confirmed to contain Ru2+ and possess the Ru-PNP-CO-diCl structure (Scheme 1).

The conversion of CO_2 to formic acid is thermodynamically favorable in alkaline aqueous solutions, and recent studies have reported the use of various tertiary amines as bases (Table S1). Among these, triethylamine was selected as the base for catalytic activity analysis due to its common use in conventional heterogeneous catalysts, facilitating a comparison of activity between conventional catalysts and the **1** catalyst.[13, 44] For the catalytic activity evaluation, standard hydrogenation conditions (120 °C, 80 bar, 3 M TEA, 10 mg cat. amount) were employed with either Ru nanoparticles on activated carbon (RuNP@AC) or the CTF catalyst with NN-based ligand motif ($RuCl_3$@$TN_{20}Bpy_1$-CTF) (Table 1, entries 1–2, 6) for comparison. RuNP@AC demonstrated a productivity of 130 $kg_{formate}/(kg_{catalyst}\cdot d)$, producing 0.12 M formate over a reaction time of 120 minutes (Table 1, entry 1). Using $RuCl_3$@$TN_{20}Bpy_1$-CTF, which has been previously reported to possess excellent catalytic activity and stability, the reaction produced 0.61 M of formate in 120 minutes, corresponding to a productivity of 670 $kg_{formate}/(kg_{catalyst}\cdot d)$.[13] This result is very similar to the previously reported catalytic activity values. These preliminary results confirm that the hydrogenation reaction conditions reported here are capable of reproducing previously obtained results. The synthesized **1** exhibited remarkable activity, generating 1.01 M of formate in only 10 minutes (Table 1, entry 6). When converted to productivity, this result is 13,400 $kg_{formate}/(kg_{catalyst}\cdot d)$, indicating a more than 20-fold increase in catalytic activity compared to the conventional CTF catalyst.

To assess the activity of the **1** catalyst relative to the homogeneous Ru-MACHO catalyst, the latter was evaluated in CO_2 hydrogenation under identical conditions (120 °C, 80 bar, 10 min), resulting in the production of 1.14 M formate (Table 1, entry 3). The heterogeneous **1** catalyst, which produced 1.01 M formate under the same conditions (Table 1, entry 6), demonstrated 90% of the activity of its homogeneous counterpart,

Table 1. Catalytic activity for Formate Production via Carbon Dioxide Hydrogenation Using Selected Hydrogenation Catalysts.[a]

Entry	Catalyst.	*T* [°C]	Total P[b] [bar]	Gas ratio [H_2:CO_2]	Format [M]	Productivity [$kg_{formate}/(kg_{catalyst}\cdot d)$]
1[c]	RuNP@AC	120	80	1:1	0.12	130
2[c]	$RuCl_3$@$TN_{20}Bpy_1$-CTF	120	80	1:1	0.61	670
3[d]	Ru-MACHO	120	80	1:1	1.14	-
4	**1**	80	80	1:1	0.10	1,260
5	**1**	100	80	1:1	0.42	5,500
6	**1**	120	80	1:1	1.01	13,400
7	**1**	140	80	1:1	0.98	13,000
8	**1**	160	80	1:1	0.96	12,700
9	**1**	120	20	1:1	0.22	2,890
10	**1**	120	40	1:1	0.48	6,360
11	**1**	120	80	1:3	0.66	8,780
12	**1**	120	80	3:1	1.28	17,000
13[e]	**1**	120	80	3:1	0.82	36,100
14[f]	**1**	120	80	3:1	2.11	9,300

[a] Reaction conditions: Ru-MACHO-POMP (**1**) (10 mg, 10.3 μmol Ru), triethyl amine (TEA, 6.1 g, 8.4 mL, 60 mmol), H_2O (11.6 mL), 8 MPa (CO_2:H_2 = 1:1), 120 °C, 10 min. [b] Total pressure at room temperature, [c] 120 min. [d] 10.3 μmol was used. [e] 3 min. [f] 30 min.

© 2024 The Authors. ChemSusChem published by Wiley-VCH GmbH

1864564x, 2025, 5, Downloaded from https://chemistry-europe.onlinelibrary.wiley.com/doi/10.1002/cssc.202402038 by Chung-Ang University, Wiley Online Library on [11/05/2026]. See the Terms and Conditions (https://onlinelibrary.wiley.com/terms-and-conditions) on Wiley Online Library for rules of use; OA articles are governed by the applicable Creative Commons License

confirming that the high potential activity of the homogeneous catalyst was effectively transferred and maintained in the heterogeneous form.

The formate production reaction through CO_2 hydrogenation is known to be influenced by various reaction conditions including temperature, pressure, and hydrogen partial pressure ratio. The conditions influencing the hydrogenation of CO_2 using **1** were evaluated, and the process was optimized by conducting catalyst activity tests under various reaction conditions (Table 1, entry 4–14). First, experiments were conducted to observe the catalytic activity as a function of temperature (Table 1, entry 4–8). The activity rate of the catalyst exhibited a marked increase when the temperature was increased from 80 to 120 °C, culminating in a peak with a productivity of 13,400 $kg_{formate}/(kg_{catalyst}\cdot d)$ at 120 °C (Table 1, entry 4–6). However, at 140 and 160 °C, there was no significant increase in activity; instead, a slight decrease in productivity value of 13,000 and 12,700 $kg_{formate}/(kg_{catalyst}\cdot d)$, respectively, was observed (Table 1, entry 7–8). This highlights 120 °C as the optimal temperature for the highest catalytic activity.

Secondly, pressure dependency was assessed by maintaining the optimal temperature at 120 °C and varying the pressure (Table 1, entry 6, 9–10), which revealed a linear increase in the productivity values of 2,890, 6,360, and 13,400 $kg_{formate}/(kg_{catalyst}\cdot d)$ at overall pressures of 20, 40, and 80 bar, respectively. This indicates a proportional relationship between catalytic activity and pressure.

Finally, the dependence on the H_2 and CO_2 partial pressures was examined by altering the H_2:CO_2 ratio to 1:3 and 3:1 during hydrogenation (Table 1, entry 11–12). A reduced productivity of 8,780 $kg_{formate}/(kg_{catalyst}\cdot d)$ was obtained using a 1:3 ratio (H_2:CO_2) instead of a 1:1 ratio, whereas an increased productivity of 17,000 $kg_{formate}/(kg_{catalyst}\cdot d)$ was obtained using a 3:1 ratio (H_2:CO_2). Thus, it was observed that the reaction rate increased with a higher relative hydrogen partial pressure compared to the amount of CO_2. These results are consistent with the established trend in CO2 hydrogenation processes using conventional Ru catalysts, where an increase in hydrogen partial pressure leads to enhanced catalytic activity. This phenomenon is generally attributed to the mechanism at the catalyst's active site, where hydrogen binds to the metal and forms a metal hydride through heterolytic cleavage, serving as the rate-determining step in the CO_2 hydrogenation reaction (Figure S5).[54, 76] Based on these experimental results, the optimized conditions for **1** were determined to be 120 °C and 80 bar with a hydrogen to carbon dioxide ratio of 3:1.

To determine the turnover frequency (TOF), which is considered a critical indicator of catalyst efficiency and performance in heterogeneous catalysts, representing the number of reactions occurring at a single active site per unit time, the amount of formic acid produced over varying reaction times under optimized conditions was measured (Figure 2, a, Table 1, entry 6, 13–14). The results showed the production of 0.82 M formate in 3 min and 2.11 M in 30 min. Therefore, the initial TOF value of **1** was determined to be 31,700, calculated from the formation of 0.82 M in 3 min.

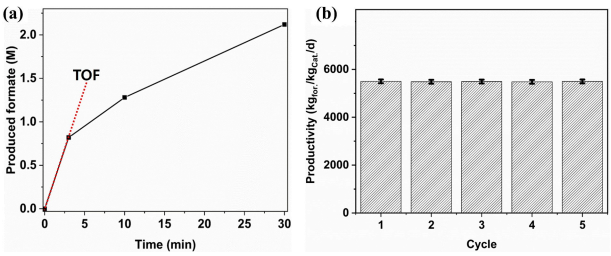


Figure 2. (a) Graph of formate production per hour; (b) Formate productivity in recyclability experiments of the **1**.

To explore the recyclability of the catalyst, a series of recycling experiments was conducted (Figure 2b). The catalyst, with a size exceeding 20 μm (Figure 1a), was easily separated from the reaction mixture by simple filtration and reused in hydrogenation reactions without additional treatment. Remarkably, activity and productivity were maintained after five cycles, indicating that **1** possesses the excellent durability required for a heterogeneous catalyst. Additionally, the catalyst recovered after four times recycle was analyzed using ICP-OES, and no change in Ru content (wt%) was observed compared to as-prepared **1**.

The CCU technology that generates value-added products through CO_2 hydrogenation must ultimately be applied at an industrial scale for mass production to meaningfully contribute to climate change mitigation. For the developed catalysts to be suitable for large-scale production of formic acid, they require not only stability but also high catalytic activity.[13, 16] Prior studies on heterogeneous catalyst for CO_2 hydrogenation have mainly aimed at enhancing catalytic activity and have reported excellent TOF values. However, in large-scale industrial processes, along with the TOF, productivity ($kg_{formate}/(kg_{catalyst}\cdot d)$) plays a crucial role in evaluating and optimizing the practical performance of catalysts. Therefore, the industrial applicability of the developed catalyst **1** was assessed by comparing its productivity with one of reported Ru catalysts (Figure 3).[13, 44] Additionally, as the weight of formate produced varies with the

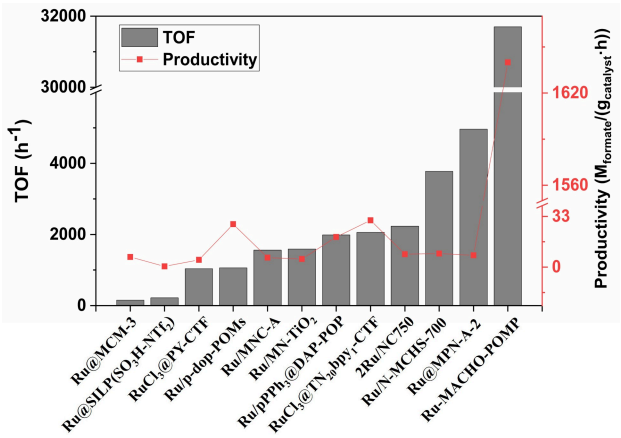


Figure 3. Graphs comparing the TOF and productivity of reported catalysts and **1**.[13, 44]

© 2024 The Authors. ChemSusChem published by Wiley-VCH GmbH

1864564x, 2025, 5, Downloaded from https://chemistry-europe.onlinelibrary.wiley.com/doi/10.1002/cssc.202402038 by Chung-Ang University, Wiley Online Library on [11/05/2026]. See the Terms and Conditions (https://onlinelibrary.wiley.com/terms-and-conditions) on Wiley Online Library for rules of use; OA articles are governed by the applicable Creative Commons License

type of base used, productivity was expressed in terms of the molar concentration of formate [$M_{formate}/(g_{cat}\cdot h)$] for generalization, and these productivity values were calculated based on the highest TOF values reported in the literature. In the last five years, reported Ru catalysts have demonstrated TOFs of up to 5,000, while **1** exhibited a significantly higher initial TOF of 31,700. Furthermore, it was observed that for some catalysts, the reported TOF and the calculated productivity are not correlated, due to the low proportion of active sites relative to the total mass of the catalyst. In contrast, **1** being a heterogenized catalyst formed with a homogeneous catalyst using a -CH_2- linker, exhibited a very high concentration of active sites (> 63 wt%) relative to its mass, resulting in a record high productivity of 1,640 $M_{formate}/(g_{cat}\cdot h)$. The results indicate that the developed catalyst **1** has high potential for industrial application in formic acid production through CO_2 hydrogenation.

Conclusions

In conclusion, the synthesis and characterization of Ru-MACHO-POMP as a heterogeneous catalyst for CO_2 hydrogenation to formate have been successfully demonstrated. The catalyst was prepared via a solvothermal method, resulting in stable particles with a uniform distribution of active Ru sites. Various analytical techniques confirmed the successful heterogenization of the Ru-MACHO complex and the formation of crosslinked structures within the catalyst. The catalyst exhibited exceptional catalytic activity, achieving high formate productivity and turnover frequency, surpassing both homogeneous and heterogeneous counterparts. Optimization studies revealed the influence of reaction parameters on catalytic performance, highlighting 120 °C as the optimal temperature for maximum activity (31,700 TOF). Moreover, the catalyst demonstrated sustained activity over prolonged reaction times and maintained recyclability over multiple recycles, featuring its potential for practical applications. Comparative analysis indicated the superior performance of Ru-MACHO-POMP compared to recent Ru catalysts, emphasizing its high TOF potential and productivity. Overall, Ru-MACHO-POMP emerges as a highly promising heterogeneous catalyst with excellent catalytic activity and sustainability for CO_2 hydrogenation, offering significant prospects for the development of efficient and environmentally friendly formate production processes.

Acknowledgments

This work was supported by the DACU Project (RS-2023-00259920) and the Carbon to X Project (2020 M3H7 A1098259) through the National Research Foundation of Korea (NRF), funded by the Ministry of Science, ICT, and Future Planning, Republic of Korea. This research was supported by the Chung-Ang University Graduate Research Scholarship in 2021.

Conflict of Interests

The authors declare no conflict of interest.

Data Availability Statement

The data that support the findings of this study are available from the corresponding author upon reasonable request.

Keywords: PNP pincer type ligand · Porous organometallic polymer (POMP) · CO_2hydrogenation into formate · Exceptional productivity · Sustainable recyclability

[1] A. Gunther, A. Barthelmes, V. Huth, H. Joosten, G. Jurasinski, F. Koebsch, J. Couwenberg, *Nat. Commun.* **2020**, *11*, 1644.
[2] A. Mikhaylov, N. Moiseev, K. Aleshin, T. Burkhardt, *Entrepreneur. Sustain. Iss.* **2020**, *7*, 2897–2913.
[3] K. O. Yoro, M. O. Daramola, *Adv. Carbon Capture* **2020**, 3–28.
[4] M. Klöwer, M. R. Allen, D. S. Lee, S. R. Proud, L. Gallagher, A. Skowron, *Environ. Res. Lett.* **2021**, *16*, 104027.
[5] A. Rehman, M. M. Alam, I. Ozturk, R. Alvarado, M. Murshed, C. Isik, H. Ma, *Environ. Sci. Pollut. Res. Int.* **2023**, *30*, 9699–9712.
[6] W. Gao, S. Liang, R. Wang, Q. Jiang, Y. Zhang, Q. Zheng, B. Xie, C. Y. Toe, X. Zhu, J. Wang, L. Huang, Y. Gao, Z. Wang, C. Jo, Q. Wang, L. Wang, Y. Liu, B. Louis, J. Scott, A. C. Roger, R. Amal, H. He, S. E. Park, *Chem. Soc. Rev.* **2020**, *49*, 8584–8686.
[7] M. A. Sabri, S. Al Jitan, D. Bahamon, L. F. Vega, G. Palmisano, *Sci. Total Environ.* **2021**, *790*, 148081.
[8] M. Mariyaselvakumar, G. G. Kadam, M. Mani, K. Srinivasan, L. J. Konwar, *J. CO2 Utiliz.* **2023**, *67*, 102326.
[9] W. Wang, S. Wang, X. Ma, J. Gong, *Chem. Soc. Rev.* **2011**, *40*, 3703–3727.
[10] A. Alvarez, A. Bansode, A. Urakawa, A. V. Bavykina, T. A. Wezendonk, M. Makkee, J. Gascon, F. Kapteijn, *Chem. Rev.* **2017**, *117*, 9804–9838.
[11] Z. Wang, Y. Kang, J. Hu, Q. Ji, Z. Lu, G. Xu, Y. Qi, M. Zhang, W. Zhang, R. Huang, L. Yu, Z. Q. Tian, D. Deng, *Angew. Chem. Int. Ed. Engl.* **2023**, *62*, e202307086.
[12] C. Wu, D. Wang, J. Guo, A. Zavabeti, P. Xiao, G. K. Li, *Energy and Fuels* **2024**, *38*, 3357–3368.
[13] K. Park, G. H. Gunasekar, S.-H. Kim, H. Park, S. Kim, K. Park, K.-D. Jung, S. Yoon, *Green Chem.* **2020**, *22*, 1639–1649.
[14] H. Yoon, T. Yoon, H.-J. Yoon, C.-J. Lee, S. Yoon, *Green Chem.* **2022**, *24*, 1738–1745.
[15] H. Yoon, T. Yoon, C.-J. Lee, S. Yoon, *Chem. Eng. J.* **2023**, *469*, 143684.
[16] C. Kim, K. Park, H. Lee, J. Im, D. Ususky, K. Tak, D. Park, W. Chung, D. Han, J. Yoon, H. Lee, H. Kim, Margareth, J. Jung, D. H. Won, C.-J. Yoo, K. B. Lee, K.-D. Jung, U. Lee, *Joule* **2024**, *8*, 693–713.
[17] A. H. Liu, R. Ma, C. Song, Z. Z. Yang, A. Yu, Y. Cai, L. N. He, Y. N. Zhao, B. Yu, Q. W. Song, *Angew. Chem. Int. Ed. Engl.* **2012**, *51*, 11306–11310.
[18] P. G. Jessop, T. Ikariya, R. Noyori, *Chem. Rev.* **1995**, *95*, 259–272.
[19] P. G. Jessop, T. Ikariya, R. Noyori, *Chem. Rev.* **1999**, *99*, 475–493.
[20] B. Loges, A. Boddien, F. Gärtner, H. Junge, M. Beller, *Top. Catal.* **2010**, *53*, 902–914.
[21] K. Sordakis, C. Tang, L. K. Vogt, H. Junge, P. J. Dyson, M. Beller, G. Laurenczy, *Chem. Rev.* **2018**, *118*, 372–433.
[22] R. Tanaka, M. Yamashita, K. Nozaki, *J. Am. Chem. Soc.* **2009**, *131*, 14168–14169.
[23] R. Tanaka, M. Yamashita, L. W. Chung, K. Morokuma, K. Nozaki, *Organometallics* **2011**, *30*, 6742–6750.
[24] J. F. Hull, Y. Himeda, W. H. Wang, B. Hashiguchi, R. Periana, D. J. Szalda, J. T. Muckerman, E. Fujita, *Nat. Chem.* **2012**, *4*, 383–388.
[25] G. A. Filonenko, R. van Putten, E. N. Schulpen, E. J. M. Hensen, E. A. Pidko, *ChemCatChem* **2014**, *6*, 1526–1530.
[26] J. Kothandaraman, M. Czaun, A. Goeppert, R. Haiges, J. P. Jones, R. B. May, G. K. Prakash, G. A. Olah, *ChemSusChem* **2015**, *8*, 1442–1451.
[27] M. Scott, B. Blas Molinos, C. Westhues, G. Francio, W. Leitner, *ChemSusChem* **2017**, *10*, 1085–1093.
[28] C. Guan, Y. Pan, E. P. L. Ang, J. Hu, C. Yao, M.-H. Huang, H. Li, Z. Lai, K.-W. Huang, *Green Chem.* **2018**, *20*, 4201–4205.

© 2024 The Authors. ChemSusChem published by Wiley-VCH GmbH

1864564x, 2025, 5, Downloaded from https://chemistry-europe.onlinelibrary.wiley.com/doi/10.1002/cssc.202402038 by Chung-Ang University, Wiley Online Library on [11/05/2026]. See the Terms and Conditions (https://onlinelibrary.wiley.com/terms-and-conditions) on Wiley Online Library for rules of use; OA articles are governed by the applicable Creative Commons License

[29] L. Ji, T. Cui, X. Nie, Y. Zheng, X. Zheng, H. Fu, M. Yuan, H. Chen, J. Xu, R. Li, *Catal. Sci. Technol.* **2021**, *11*, 6965–6969.
[30] C. Rebreyend, E. A. Pidko, G. A. Filonenko, *Green Chem.* **2021**, *23*, 8848–8852.
[31] K. Schlenker, E. G. Christensen, A. A. Zhanserkeev, G. R. McDonald, E. L. Yang, K. T. Lutz, R. P. Steele, R. T. VanderLinden, C. T. Saouma, *ACS Catalysis* **2021**, *11*, 8358–8369.
[32] D. Wei, H. Junge, M. Beller, *Chem. Sci.* **2021**, *12*, 6020–6024.
[33] C. Das, J. Grover, Tannu, A. Das, D. Maiti, A. Dutta, G. K. Lahiri, *Dalton Trans.* **2022**, *51*, 8160–8168.
[34] A. S. Tossaint, C. Rebreyend, V. Sinha, M. Weber, S. Canossa, E. A. Pidko, G. A. Filonenko, *Catal. Sci. Technol.* **2022**, *12*, 2972–2977.
[35] D. Wei, R. Sang, A. Moazezbarabadi, H. Junge, M. Beller, *JACS Au* **2022**, *2*, 1020–1031.
[36] S. Kushwaha, J. Parthiban, S. K. Singh, *Organometallics* **2023**, *42*, 3066–3076.
[37] S. Kushwaha, J. Parthiban, S. K. Singh, *ACS Omega* **2023**, *8*, 38773–38793.
[38] M. Hirano, K. Wada, H. Matsuda, E. A. Pidko, *J. CO2 Utiliz.* **2024**, *81*, 102718.
[39] M. D. Morton, B. Y. Tay, J. J. Q. Mah, A. J. P. White, J. D. Nobbs, M. van Meurs, G. J. P. Britovsek, *Inorg. Chem.* **2024**, *63*, 3393–3401.
[40] D. J. Cole-Hamilton, *Science* **2003**, *299*, 1702–1706.
[41] I. Vural Gürsel, T. Noël, Q. Wang, V. Hessel, *Green Chem.* **2015**, *17*, 2012–2026.
[42] A. Agapova, H. Junge, M. Beller, *Chemistry* **2019**, *25*, 9345–9349.
[43] F. Zaera, *Chem. Rev.* **2022**, *122*, 8594–8757.
[44] B. Chen, M. Dong, S. Liu, Z. Xie, J. Yang, S. Li, Y. Wang, J. Du, H. Liu, B. Han, *ACS Catal.* **2020**, *10*, 8557–8566.
[45] A. Jaleel, S.-H. Kim, P. Natarajan, G. H. Gunasekar, K. Park, S. Yoon, K.-D. Jung, *J. CO2 Utiliz.* **2020**, *35*, 245–255.
[46] Q. Wang, S. Santos, C. A. Urbina-Blanco, W. Y. Hernández, M. Impéror-Clerc, E. I. Vovk, M. Marinova, O. Ersen, W. Baaziz, O. V. Safonova, A. Y. Khodakov, M. Saeys, V. V. Ordomsky, *Appl. Catal. B Environ.* **2021**, *290*, 120036.
[47] S. Ahn, K. Park, K. R. Lee, A. Haider, C. V. Nguyen, H. Jin, S. J. Yoo, S. Yoon, K.-D. Jung, *Chem. Eng. J.* **2022**, *442*, 136185.
[48] A. Jaleel, A. Haider, C. V. Nguyen, K. R. Lee, S. Choung, J. W. Han, S.-H. Baek, C.-H. Shin, K.-D. Jung, *Chem. Eng. J.* **2022**, *433*, 133571.
[49] S. J. Louis Anandaraj, L. Kang, S. DeBeer, A. Bordet, W. Leitner, *Small* **2023**, *19*, e2206806.
[50] M. Luo, X. Hu, Z. Fan, S. Ma, G. Song, L. Jin, C. Jie, S. Wang, *Chem. Eng. J.* **2023**, *474*, 145622.
[51] K. Park, K. R. Lee, S. Ahn, S.-H. Kim, A. Haider, S. Choung, J. W. Han, K.-D. Jung, *Appl. Catal. B Environ.* **2023**, *335*, 122873.
[52] K. Park, K. R. Lee, S. Ahn, C. V. Nguyen, K.-D. Jung, *Appl. Catal. B: Environ. Energy* **2024**, *346*, 123751.
[53] G. Ji, C. Li, B. Fan, G. Wang, Z. Sun, M. Jiang, L. Ma, L. Yan, Y. Ding, *ACS Catal.* **2024**, *14*, 1595–1607.
[54] J. B. Curley, C. Hert, W. H. Bernskoetter, N. Hazari, B. Q. Mercado, *Inorg. Chem.* **2022**, *61*, 643–656.
[55] A. Moazezbarabadi, D. Wei, H. Junge, M. Beller, *ChemSusChem* **2022**, *15*, e202201502.
[56] R. I. Walton, *Chem. Soc. Rev.* **2002**, *31*, 230–238.
[57] F. Ahmadijokani, H. Molavi, M. Rezakazemi, S. Tajahmadi, A. Bahi, F. Ko, T. M. Aminabhavi, J.-R. Li, M. Arjmand, *Progr. Mater. Sci.* **2022**, *125*, 100904.
[58] Y. Huo, S. Xiu, L.-Y. Meng, B. Quan, *Chem. Eng. J.* **2023**, *451*, 138572.
[59] V. Rozyyev, Y. Hong, M. S. Yavuz, D. Thirion, C. T. Yavuz, *Adv. Energy Sustain. Res.* **2021**, *2*, 2100064.
[60] V. Ganesan, S. Yoon, *ACS Appl. Mater. Interf.* **2019**, *11*, 18609–18616.
[61] G. H. Gunasekar, S. Yoon, *J. Mater. Chem. A* **2019**, *7*, 14019–14026.
[62] J. Jiang, S. Yoon, *J. Mater. Chem. A* **2019**, *7*, 6120–6125.
[63] V. Ganesan, S. Yoon, *Inorg. Chem.* **2020**, *59*, 2881–2889.
[64] K. Park, S. Padmanaban, S. H. Kim, K. D. Jung, S. Yoon, *ChemCatChem* **2020**, *13*, 695–703.
[65] S. Padmanaban, G. H. Gunasekar, S. Yoon, *Inorg. Chem.* **2021**, *60*, 6881–6888.
[66] H. Park, K. Park, K.-D. Jung, S. Yoon, *Inorg. Chem. Front.* **2021**, *8*, 1727–1735.
[67] Q. Wang, M. Unno, H. Liu, *Materials (Basel)* **2021**, *14*, 3851.
[68] S. Hou, J. Hu, X. Liang, D. Zhang, B. Tan, *J. Mater. Chem. A* **2022**, *10*, 15062–15073.
[69] S. Padmanaban, V. Ganesan, S. Yoon, Y. Lee, *Inorg. Chem.* **2022**, *61*, 1552–1561.
[70] H. Zhou, C. Rayer, A. R. Antonangelo, N. Hawkins, M. Carta, *ACS Appl. Mater. Interf.* **2022**, *14*, 20997–21006.
[71] J. Wang, T. Wu, X. Wang, J. Chen, M. Fan, Z. Shi, J. Liu, L. Xu, Y. Zang, *iScience* **2024**, *27*, 108993.
[72] K. Jarzembska, S. Seal, K. Woźniak, A. Szadkowska, M. Bieniek, K. Grela, *ChemCatChem* **2009**, *1*, 144–151.
[73] D. J. Morgan, *Surf. Interf. Anal.* **2015**, *47*, 1072–1079.
[74] H. Park, S. Yoon, *ACS Sustain. Chem. Eng.* **2023**, *11*, 12036–12044.
[75] C. Armstrong, J. A. J. Burnham, E. E. Warminski, *J. Chem. Educ.* **2017**, *94*, 928–931.
[76] S. Ogo, R. Kabe, H. Hayashi, R. Harada, S. Fukuzumi, *Dalton Trans.* **2006**, 4657–4663.

Manuscript received: October 8, 2024
Revised manuscript received: October 14, 2024
Accepted manuscript online: October 14, 2024
Version of record online: November 27, 2024

© 2024 The Authors. ChemSusChem published by Wiley-VCH GmbH

1864564x, 2025, 5, Downloaded from https://chemistry-europe.onlinelibrary.wiley.com/doi/10.1002/cssc.202402038 by Chung-Ang University, Wiley Online Library on [11/05/2026]. See the Terms and Conditions (https://onlinelibrary.wiley.com/terms-and-conditions) on Wiley Online Library for rules of use; OA articles are governed by the applicable Creative Commons License